Military Technical College
Kobry El-Kobbah,
Cairo, Egypt.

17th International Conference on Applied Mechanics and Mechanical Engineering.

EFFECT OF GTA WELDING PARAMETERS ON MECHANICAL AND CORROSION PROPERTIES OF 254SMO SUPERAUSTENITIC STAINLESS STEEL

A. El-Batahgy[a], I. Hamed[b] and H. Hussein[c]

ABSTRACT

The current work is concentrated on scientific and deep understanding of GTA welding of 254SMO superaustenitic stainless steel. In this regard, influence of different GTA welding parameters on size and microstructure of weld zone then, on mechanical and corrosion properties of the concerned steel welded joints was clarified. Both bead-on-plate and butt welded joints were made. Welded joints were subjected to visual, dye penetrant and radiography tests before sectioning it for different destructive tests. Accelerated corrosion test was carried out based on tafel plot technique.

The results achieved in this investigation disclosed that welding parameters played an important role in obtaining acceptable weld profile. Lower welding current and/or lower oxygen content in purging gas resulted in better weld profile with smaller weld zone due to lower heat input. Besides, acceptable mechanical and corrosion properties were obtained in comparison with that of base metal.

Mechanical propertied of GTA welded joints were not significantly affected by either welding current or oxygen content in purging gas since the used base metal is not susceptible to hardening due to welding.

On the other hand, corrosion rate increased with the increase in welding current and/or oxygen content in purging gas. This is related to the increase in weld zone size due to higher heat input in this case. This means that GTA welded joint made using lower welding current and/or lower oxygen content in purging gas with smaller fusion zone size has better mechanical properties as well as corrosion resistance.

KEYWORDS

Superaustenitic stainless steel, GTA welding, Welding current, Oxygen content in purging gas, Mechanical properties, Corrosion resistance.

---

[a] Manufacturing Technology Department, Central Metallurgical R & D Institute, Cairo, Egypt (elbatahgy@yahoo.com)
[b] Chemical Engineering Department, El-Menya University, El-Menya, Egypt.
[c] Oil and Gas Company, Khafji Joint Operation, Penspen, KSA.

INTRODUCTION

Austenitic stainless steels are widely used in many industrial applications, mainly due to their good corrosion resistance. 316L stainless steel is one of the most popular austenitic stainless steel used for desalination plants and offshore facilities. The 316/316L stainless steels include Molybdenum which makes the passive layer tougher and more adherent, thereby increasing the material's resistance to pitting in reducing environments (1). Super-austenitic stainless steel 254SMO UNS 31254 was developed to overcome the conventional austenitic stainless steels corrosion problems without severe losses in mechanical properties (2-4).

The excellent corrosion resistance of Type 254SMO stainless steel in chloride solution is due to the presence of high Mo content and synergistic action of its alloying elements (5-7). In common with all austenitic stainless steels including 254SMO have low thermal conductivity and high thermal expansion. Then, welding should be carefully planned in advance so that distortion of the welded joint can be minimized.

Fusion welding is one of the most employed methods of fabricating superaustenitic stainless steels components (8-10). Due to the intense heat input, many problems arise and welding parameters have been shown to exhibit a significant effect on weld metal composition, segregation behavior and corrosion resistance. Since the welded joint is generally the weakest part in the components, the processing parameters used during welding must be carefully controlled in order to ensure the deposition of welds that do not corrode easily or experience solidification cracking (11-16).

Since the welds are more sensitive to corrosion, it is important for understanding the factors, which affect the weldability of those materials to the successful implementation. Previous investigations have demonstrated that mechanical properties and corrosion resistance of both weld and heat affected zones are function of different welding parameters. However, this research area has not yet completed and more work is required for understanding the effect of welding current and oxygen content in the back purging gas on properties of austenitic stainless steels weldments.

EXPERIMENTAL WORK

The used base metal is a commercial superaustenitic stainless steel 254SMO with 6.4mm thickness as well as chemical composition and mechanical properties given in Table 1.

Both bead-on-plate and single-V butt welds were made using TIG welding process. Bead-on- plate welds were made using 150×100x6.4mm specimens. Schematic illustrations of TIG butt weld joint are shown in Figure 1. Weld specimens of 100×100×6.4mm were prepared as single-V butt joints with machined surfaces and were held firmly using fixture to prevent distortion. Welding was carried out in flat position using TIG welding parameters given in Table 2. Ni-base alloy ERNiCrMo-3 with 2mm diameter was used as a filler metal according to AWS A4.14 (96). Effect of heat input as a function of welding current was studied by changing welding current

between 100 and 150A that resulted in heat input in the range of 0.57-1.03 kJ/mm. Also, effect of oxygen content in purging gas was clarified by changing it in the range of 0.05 and 0.5%. The travel speed was adopted to 14cm/min to avoid excessive weld deposit. Other welding parameters were kept constant including 15 l/min argon shielding and 10 l/min argon back shielding. Stainless steel brush was used to remove any slag before depositing the next pass. The inter-pass temperature was maintained at 140℃ to avoid variations in the cooling rate among the passes. Thereafter welded samples were allowed to cool in air.

Table 1 Chemical composition and mechanical properties of the used 254SMO base metal.

Chemical Composition.

Material	C%	Si	Mn	P	S	Cr	Ni	Mo	Cu	Ti	Fe
Used BM	0.007	0.45	0.4	0.0	0.0	20.1	17.1	6.96	0.69	0.18	53.7
254SMO Standard	0.02	0.80	1.0	0.03	0.01	19.5-20.5	17.5-18.5	6.0-6.5	0.5-1.0	--	Bal.

Mechanical Properties.

Material	Yield Strength. MPa	Tensile Strength, MPa	Elongation, %
Used BM	440	750	52
254SMO Standard	340	650	35

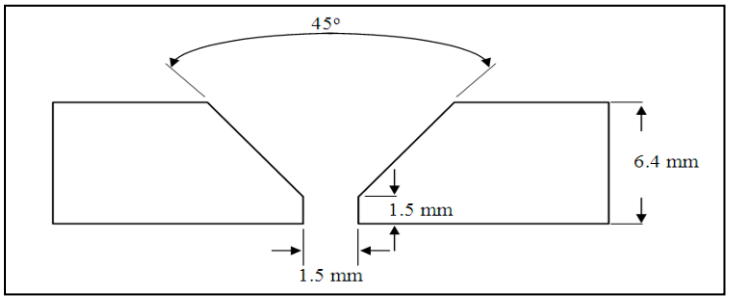

Figure 1. Schematic illustration of single V-groove butt weld joint.

Table 2. TIG welding parameters studied.

Welding current (A)	**Welding Voltage (V)**	**Welding speed cm/min**	**Shielding gas (Ar)**	**Backing gas (Ar)**	**Oxygen content(%)**	**Heat input (kJ/mm)**
100, 125, 150	14	14	15 l/min Argon	10 l/min Argon	0.05, 0.5	0.57, 0.87, 1.03

After welding, joints were inspected first using different non-destructive methods including visual, dye penetrant and radiography tests. Both visual and dye penetrant tests were carried out to check external welding defects such as surface porosity, surface crack, undercut, overlap. Then, accepted joints were subjected to radiography test to check internal welding defects such as internal porosity, internal cracks and lack of fusion or incomplete penetration.

Based on results of non-destructive tests, , accepted welded joints were sectioned and subjected to different destructive tests as shown schematically in Figure 2. Chemical analysis of welded joints was conducted using Emission Arc Spark Spectrometer (SPECTROLAB M5).

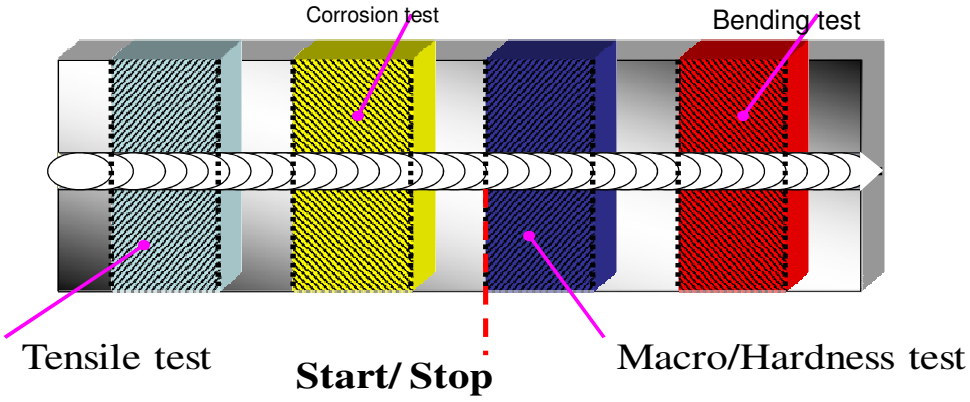

Figure 2. Schematic illustration of welded joint showing sections taken for different examinations.

Both macro- and microscopic examinations were carried out for cross sections taken from welded specimens. The aim of macro-examination is to clarify the size of weld metal as well as width of heat affected zone. Microscopic examinations were carried to clarify the microstructure of weld metal, heat affected zone and base metal. In this regard, the specimens were prepared using standard grinding, polishing and etching techniques. In other words, specimens used for metallographic examination were ground with emery paper ranging in fineness from 180 up to 1500 equivalent mesh, then polished with alumina suspension. Electrolytically etching was carried out using 10% oxalic acid solution in order to reveal the grain structure of weld metal, heat affected zone and base metal. Microscopic examination for weld metal, heat affected zone and base metal was carried out using optical microscope-Nikon Epiphot 300.

Measurements of microhardness of welded joints were carried out using Vickers hardness (HV) tester under a 200g load for 15 sec on cross-sections cut from polished and etched specimens. for hardness measurements of weld metal (WM), heat affect zone (HAZ) and base metal (BM) of welded joints. The given hardness values are the average of five readings.

Bending and tensile tests were performed for welded specimens sectioned transverse to the welding direction, at room temperature according to relevant standards (American Welding Standard). U-bend test was made for both weld face and weld root sides. In this concern, both weld and heat-affected zone of bend test specimen to be completely located within the bent portion of the specimen. Tensile

test was performed for two samples in each condition and the data reported are the average of the two individual results. Dimensions of used tensile test specimen are shown in Figure 3. The tensile test specimens were prepared in such a way that the entire weld region (weld metal, heat-affected zone and base metal) is located at the middle of specimen's gauge section. Tensile test was conducted using 100 ton electro-mechanically controlled SHIMADZU universal testing machine.

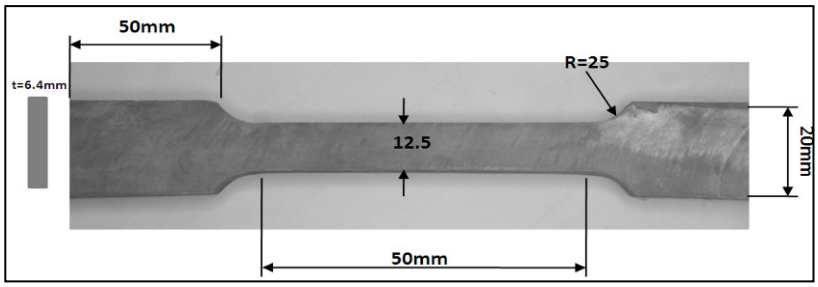

Figure 3. Dimensions of tensile test specimen.

Different welded samples were subjected to accelerated corrosion test based on tafel plot technique where corrosion rate was measured using potentiostat-Auto Lab PGSTAT 30 device. In this context, specimens were subjected to 3.5% sodium chloride under open circuit condition for 30 minutes until E-corr becomes constant. Then, potential is passed through the specimen for another 30 minutes to measure the relation between potential and current, from which corrosion rate is, deduced.

RESULTS AND DISCUSSION

Bead-on-Plate Welds

Examples of photographs of weld face and macrographs of cross sections of GTA bead-on-plate autogeneous welds made using 140mm/min welding speed, 15 l/min argon shielding, 0.05% oxygen content in purging gas and different welding currents (100, 150A) are shown in Figures 4 and 5 respectively.

Visual examination of weld face of both welds showed smooth and uniform weld bead. Visual examinations of cross sections showed incomplete penetration for both bead-on-plate welds. Macroscopic examinations of cross sections confirmed that weld penetration depth as well as HAZ width increase with increasing welding current. Weld penetration depth is increased from 3mm at 100A welding current (Figure 4-b) to 6.5mm at 150A welding current (Figure 5-b). It was reported that no welding cracks or porosity were found and this could be partly due to proper welding conditions used.

Effect of welding current on weld penetration depth has been confirmed using filler metal where weld penetration depth was increased also with increasing welding current and no welding cracks or porosity were found. In comparison with

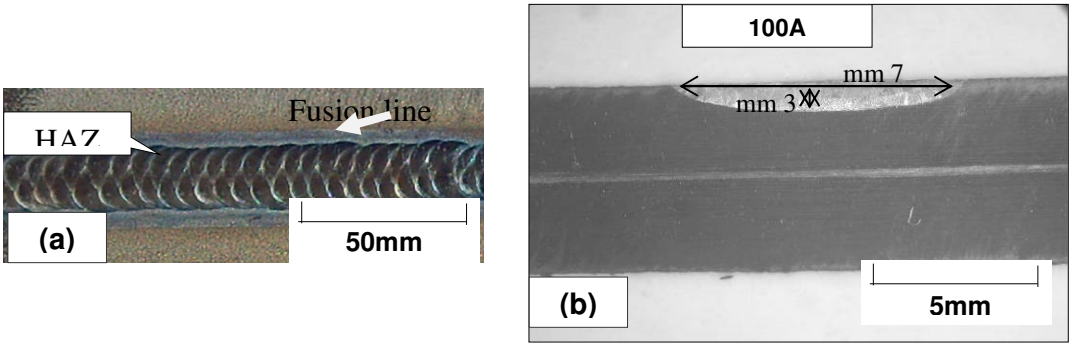

Figure 4. Photograph of face side (a) and macrograph of a cross section (b) of GTA bead-on-plate **autogeneous** weld made using **100A** welding current, 13V welding voltage, 140mm/min welding speed, 15 l/min argon flow rate, 0.05% oxygen content in back purging.

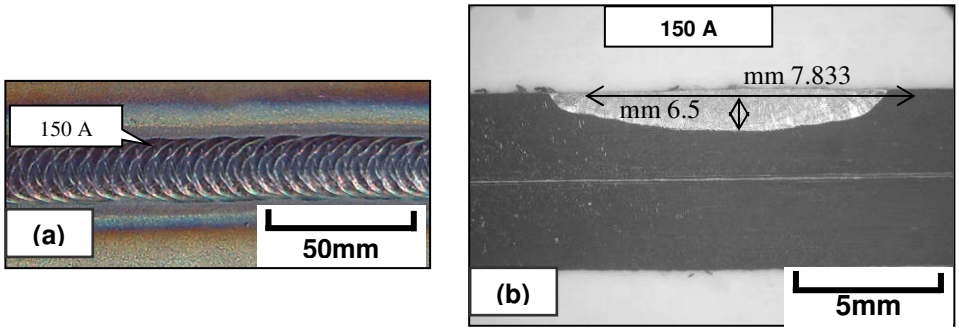

Figure 5. Photograph of face side (a) and macrograph of a cross section (b) of GTA bead-on-plate **autogeneous weld** made using **150A** welding current, 15V welding voltage, 140mm/min welding speed , 15l/min argon shielding flow rate, 0.05% oxygen content in back purging.

autogeneous welding, using filler metal has resulted in deeper weld penetration. Summary of the effect of welding current on penetration depth of bead-on-plate **autogeneous welds** made using 140mm/min welding speed, 15 l/min argon shielding and 0.05% oxygen in purging gas is shown in Figure 6. Effect of welding current on penetration depth/width ratio of bead-on-plate **autogeneous welds** of 254SMO superaustenitic stainless steel made using 140mm/min welding speed, 15 l/min argon shielding and 0.05% oxygen in purging gas is shown in Figure 7. In this regard, three different welding current (100, 125, 150A) were used with other parameters kept constant. The most important notice in Figures 6, 7 is the increase in weld penetration depth and subsequently, weld depth/width ratio with increasing welding current. The weld depth is varied with welding current as a linear relation where it increased from 3mm to 6.5mm with increasing welding current from 100A to 150A. It is seen that as the welding current increases, the weld penetration depth increases leading to higher penetration depth/width ratio that means more acceptable and stronger weld. Higher weld penetration depth (6.5mm) that corresponds to higher depth/width ratio (0.830) is obtained using 150A welding current. This is mainly due

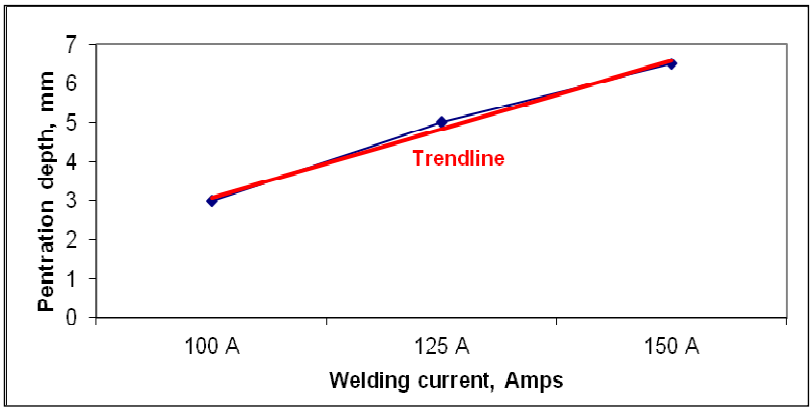

Figure 6. Effect of welding current on penetration depth of bead-on-plate **autogeneous** welds made using 140mm/min welding speed, 15 l/min argon shielding and 0.05% oxygen in purging gas.

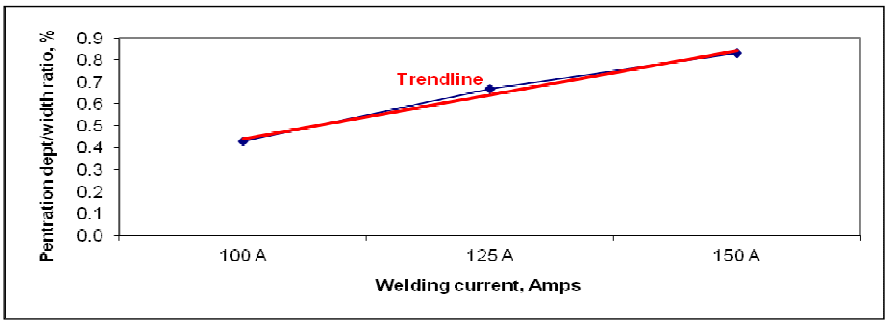

Figure 7. Effect of welding current on penetration depth/width ratio of bead-on-plate **autogeneous welds** made using 140mm/min welding speed, 15 l/min argon shielding and 0.05% oxygen in purging gas.

to proper heat input in this case. In general, it is known that high depth/width ratio of weld bead is of remarkable importance concerning metallurgical and mechanical properties and consequently stronger weld.

Summary of the effect of welding current on penetration depth of bead-on-plate welds made using **filler metal**, 140mm/min welding speed, 15 l/min argon shielding and 0.05% oxygen in purging gas is shown in Figure 8. Effect of welding current on penetration depth/width ratio of bead-on-plate welds made using **filler metal**, 140mm/min welding speed, 15 l/min argon shielding and 0.05% oxygen in purging gas is shown in Figure 9. In this regard, three different welding current (100, 125, 150A) were used with other parameters kept constant. The most important notice in Figures 8, 9 is the increase in weld penetration depth and subsequently, weld depth/width ratio with increasing welding current. The weld depth is varied with welding current as a linear relation where it increased from 4mm to 6.7mm with increasing welding current from 100A to 150A, respectively. It can be observed that

as the welding current increases, the weld penetration depth increases leading to higher penetration depth/ width ratio that means more acceptable and stronger weld. Higher weld penetration depth (6.7mm) that corresponds to higher depth/width ratio (0.628) is obtained using 150A welding current. This is mainly due to proper heat input in this case. In general, it is known that high depth/width ratio of weld bead is of remarkable importance concerning metallurgical and mechanical properties and consequently stronger weld. In comparison with autogeneous welding (Figures 6, 7), filler metal (Figures 8, 9) has resulted in deeper weld penetration and higher weld depth/width ratio.

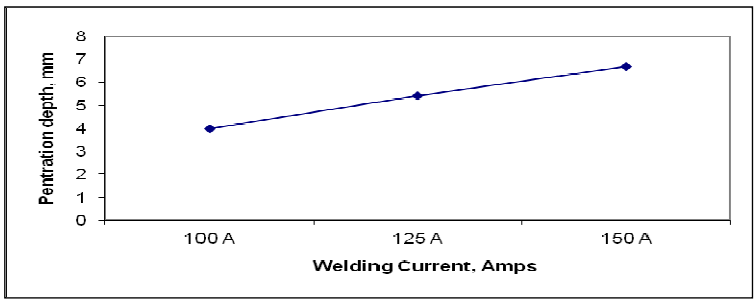

Figure 8. Effect of welding current on penetration depth of bead-on-plate welds made using **filler metal**, 140mm/min welding speed, 15 l/min argon shielding and 0.05% oxygen in purging gas.

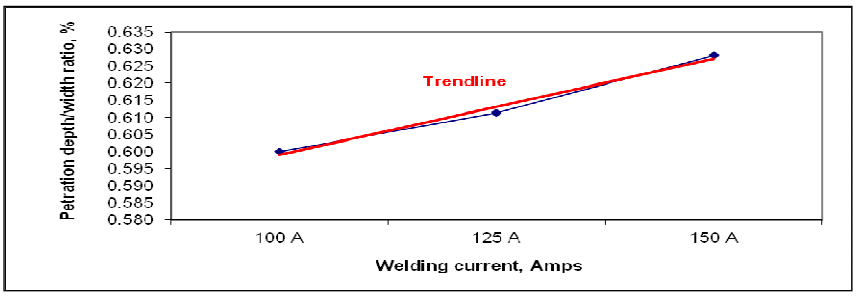

Figure 9. Effect of welding current on penetration depth/width ratio of bead-on-plate welds made using **filler metal**, 140mm/min welding speed, 15 l/min argon shielding and 0.05% oxygen in purging gas.

Butt Welded Joints

Concerning effect of welding current, photograph of face side and macrograph of cross sections of GTA butt welded joints produced using 135mm/min welding speed, 15 l/min argon shielding, 0.05% oxygen in purging gas and different welding currents (100, 150A) are shown in Figure 10 and 11 respectively. Both visual and radiographic examinations of GTA butt welded joints produced using different welding currents showed no welding defects such as porosity, undercut, cracks, incomplete penetration or lack of fusion. This may be partly due to the precise control and good reproducibility of the processing parameters selected.

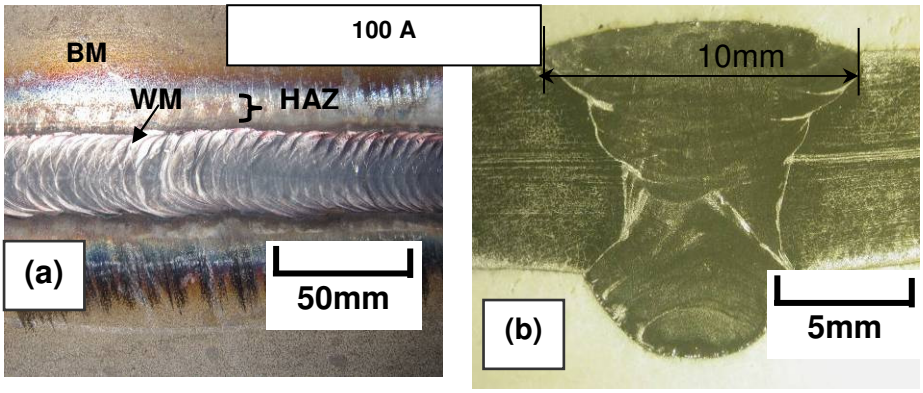

Figure 10. Photograph of face side (a) and macrograph of a cross section (b) of GTA butt welded joint produced using **100A** welding current, 13V welding voltage, 135mm/min welding speed, 15 l/min argon shielding and 0.05% oxygen in purging gas.

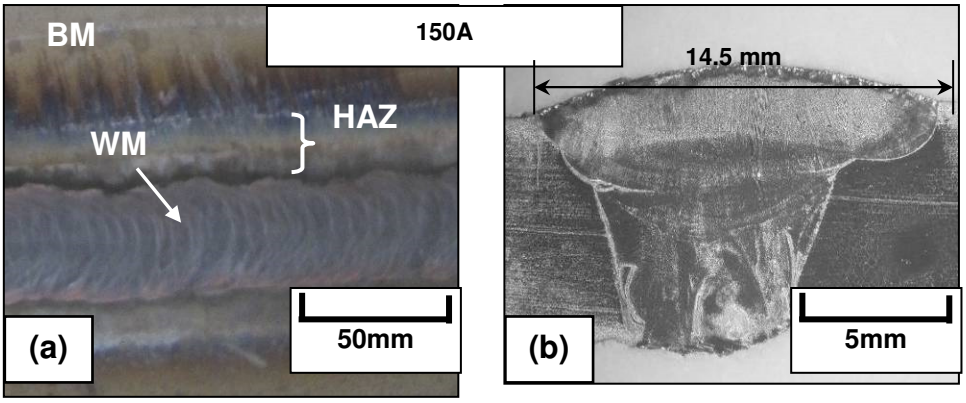

Figure 11. Photograph of face side (a) and macrograph of a cross section (b) of GTA butt welded joint produced using **150A** welding current, 15V welding voltage, 135mm/min welding speed, 15 l/min argon shielding and 0.05% oxygen in purging gas.

It can be deduced from **Figures 10, 11** that the development of the weld pool was essentially symmetrical about the axis of the electrode. Consequently, the electromagnetic force was equal to the surface tension force thereby convective heat transfer was not influenced. Visual examination of weld face showed smooth and uniform weld bead. Visual examinations of cross sections showed complete penetration for all butt welded joints. Macroscopic examinations of cross sections indicated that weld penetration width as well as HAZ width are increased with increasing welding current. Weld penetration width is increased from 10mm at 100A welding current (Figure 10) to 14.5mm at 150A welding current (Figure 11). Macroscopic examination showed no internal welding defects such as cracks or porosity and this could be partly due to proper welding conditions used.

Effect of welding current on penetration width of **butt welded joints** made using 135mm/min welding speed, 15 l/min argon shielding and 0.05% oxygen in purging gas is shown in Figure 12. Effect of welding current on penetration depth/width ratio of **butt welded joints** made using 135mm/min welding speed, 15 l/min argon shielding and 0.05% oxygen in purging gas is shown in Figure 13. In this regard, three different welding current (100, 125, 150A) were used with other parameters kept constant. The most important notice in Figures 12, 13 is the complete penetration for the full thickness (6.4mm) regardless of welding current value. Another notice is the increase in weld penetration width and subsequently, the decrease in weld depth/width ratio with increasing welding current.

The weld width and weld depth/width ratio are varied with welding current as a linear relation where weld width is increased from 10mm to14.5mm with increasing welding current from 100A to 150A, respectively. It is seen that as the welding current is increased, the weld width increases leading to lower penetration depth/ width ratio that means less acceptable weld. Lower weld width (10mm) that corresponds to higher depth/width ratio (0.64) is obtained using 100A welding current. This is mainly due to proper heat input in this case. In general, it is known that high depth/width ratio of weld bead is of remarkable importance concerning metallurgical and mechanical properties and consequently stronger weld.

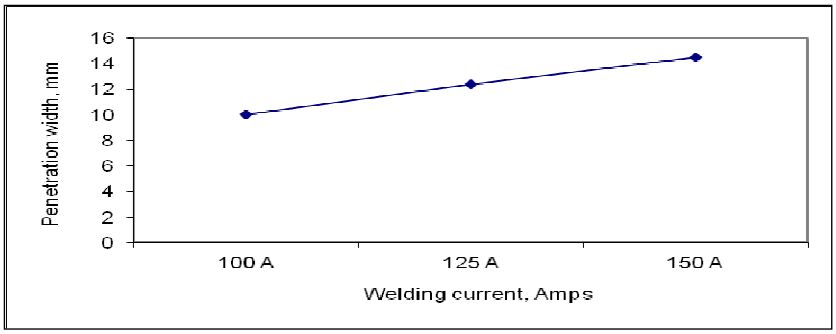

Figure 12. Effect of welding current on penetration width of **butt welded joints** made using 135mm/min welding speed, 15 l/min argon shielding and 0.05% oxygen in purging gas.

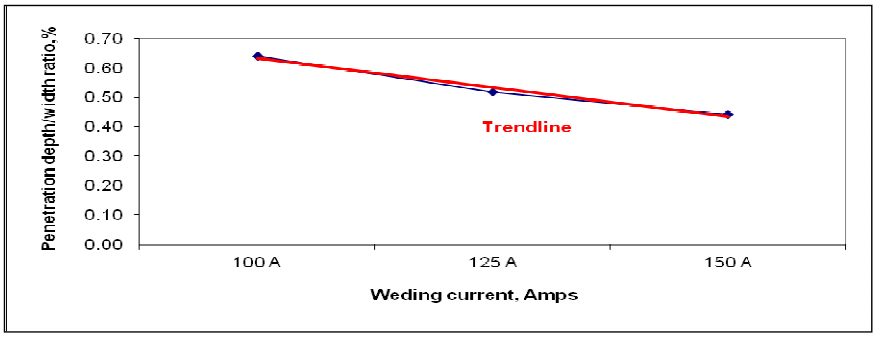

Figure 13. Effect of welding current on penetration depth/width ratio of **butt welded joints** made using 135mm/min welding speed, 15 l/min argon shielding and 0.05% oxygen in purging gas.

Regarding effect of oxygen content in purging gas, photographs of root side and macrographs of cross sections of GTA welded joint produced using 125A welding current, 14V welding voltage, 135mm/min welding speed, 15 l/min argon shielding are and different oxygen contents in purging gas (0.05, 0.5%) are shown in Figures 14 and 15 respectively.

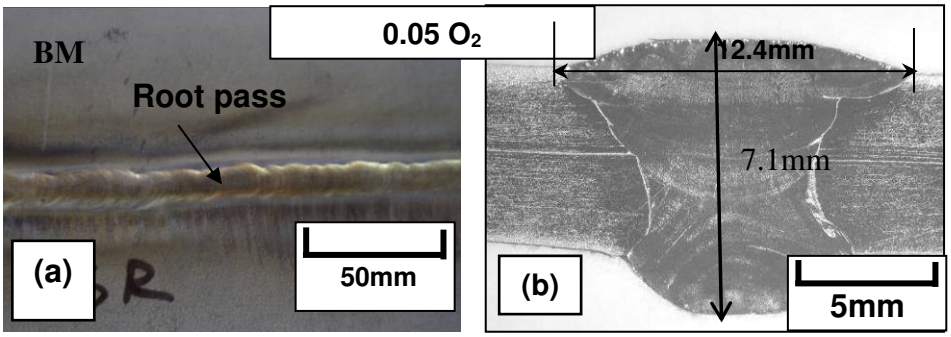

Figure 14. Photograph of root side (a) and macrograph of a cross section (b) of GTA welded joint produced using **0.05% oxygen** in purging gas, 125A welding current, 14V welding voltage and 135mm/min welding speed and 15 l/min argon shielding.

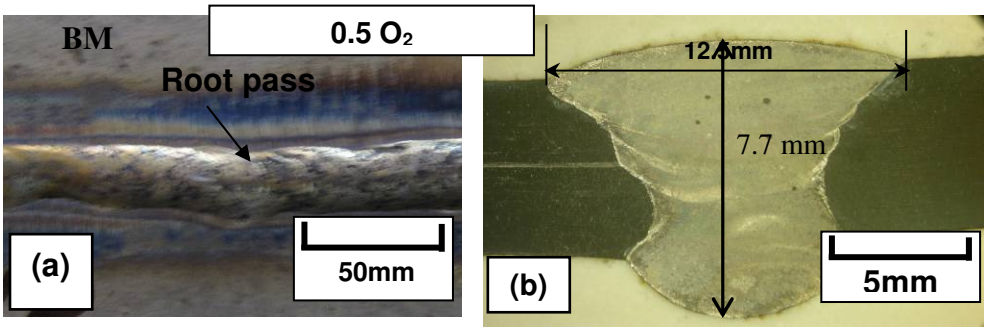

Figure 15. Photograph of root side (a) and macrograph of a cross section (b) of GTA welded joint produced using 0.5% oxygen in purging gas, 125A welding current, 14V welding voltage, 135 mm/min welding speed and 15 l/min argon shielding.

Visual examination of weld face showed smooth and uniform weld bead. Visual examinations of cross sections showed complete penetration for all butt welded joints. Macroscopic examinations of cross sections indicated that weld width and HAZ width are not affected by oxygen content in purging gas. In other words, similar weld width was obtained regardless of oxygen content in purging gas where 12.4mm weld width was obtained with 0.05% oxygen in purging gas (Figure 14-b) and 12.5mm weld width was obtained in case of 0.5% oxygen content in purging gas (Figure 15-b). Macroscopic examination showed no internal welding defects such as cracks or porosity and this could be partly due to proper welding conditions used.

Effect of oxygen content in purging gas on weld width of welded joints made using 125A welding current, 14V welding voltage, 135mm/min welding speed and 15 l/min argon shielding is shown in Figure 16. Effect of oxygen content in purging gas on penetration depth/width ratio of welded joints made using 125A welding current, 14V

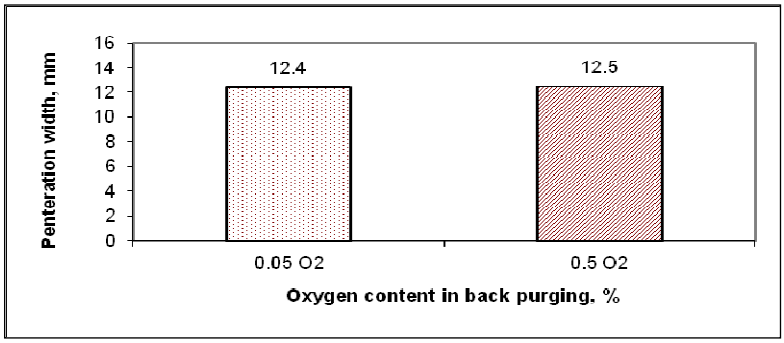

Figure 16. Effect of oxygen content in purging gas on weld width of welded joint made using 125A welding current, 14V welding voltage, 135mm/min welding speed and 15 l/min argon shielding.

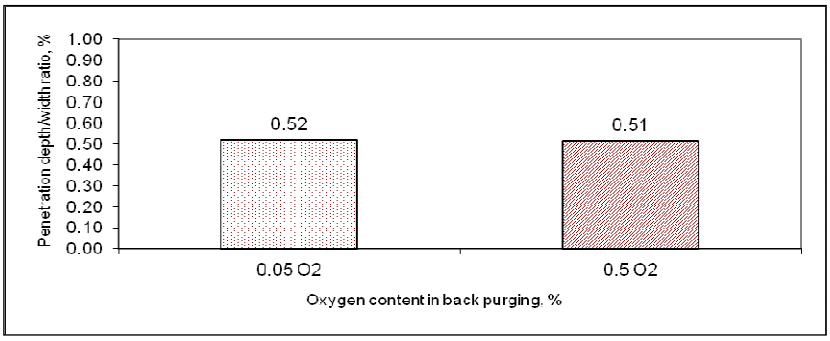

Figure 17. Effect of oxygen content in purging gas on penetration depth/width ratio of welded joint made using 125A welding current, 14V welding voltage and 135mm/min welding speed.

welding voltage, 135mm/min welding speed and 15 l/min argon shielding is shown in Figure 17.

The most important notice in Figures 16, 17 is the negligible change in weld width and subsequently, weld depth/width ratio with increasing oxygen content in purging gas. The weld width is increased from 12.4mm to 12.5mm and weld depth/width ratio is decreased from 0.52 to 0.51 with increasing oxygen content in purging gas from 0.05% to 0.5%, respectively. In other words, the oxygen content in purging gas has almost no influence on weld geometry (penetration depth, weld width, weld depth/width ratio). However, weld profile is influenced by oxygen content in purging gas. Lower oxygen content in purging gas (0.05%) has resulted in better weld profile due to narrower weld root (Figure 14) in comparison with that obtained in case of higher oxygen content in purging gas (Figure 15). This is mainly due to lower heat input in case of lower oxygen content in purging gas since lower oxygen means limited exothermic reaction. On the other hand, higher oxygen in purging gas (0.5%) results in more heat as a result of exothermic reaction. It is known that better weld profile as a result of narrower weld root is of remarkable importance concerning metallurgical and mechanical properties and consequently stronger weld.

Regarding microscopic examinations, Figure 18 shows microstructure of the used 254SMO base metal. It can be noticed that this microstructure is a typical austenitic structure for superaustenitic stainless steel 254SMO. It shows mainly austenite phase with a few percentage of delta ferrite. Usually, the austenitic region contains higher quantities of the austenite formers (nickel, manganese, carbon and nitrogen) while the ferrite region contains larger proportions of ferrite formers (chromium, iron, silicon and molybdenum). An average hardness value of about 230HV was obtained for this microstructure type.

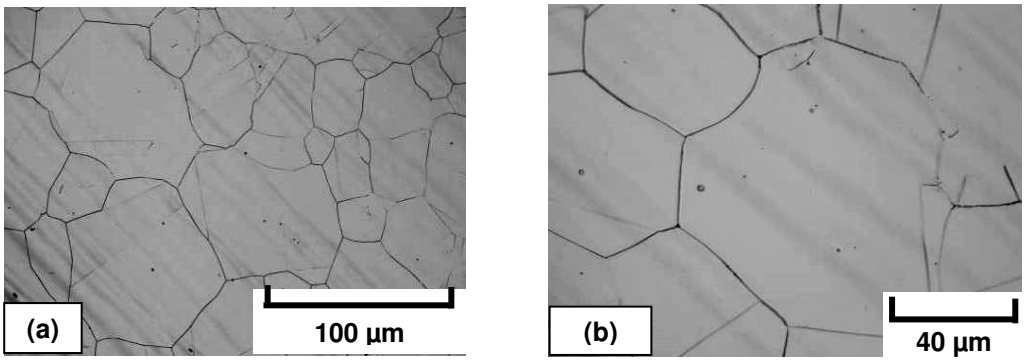

Figure 18. Optical micrographs of the used 254SMO base metal.

Optical micrographs of a cross section taken from butt welded joint produced using 135mm/min welding speed, 15 l/min argon shielding, 0.05% oxygen in purging gas and different welding currents (100, 150A) are shown in Figures 19 and 20 respectively. The noticeable feature is the directional nature of the superaustenitic microstructure around weld center of both welded joints. No solidification cracking was found in the weld zone. Structures of weld metal in both joints were almost similar where a dendritic microstructure was developed at fusion boundary due to fast cooling conditions (Figures 19c, 20-c). More globular structures were observed at weld metal center that exposed to lower cooling rates and with a less pronounced heat flow direction. The higher the welding current, the coarser is the dendritic structure due to decreasing cooling rate.

The heat affected zone (HAZ) is the area of the base metal that has its microstructure and properties altered by inducing intensive heat into the metal. HAZ microstructure is critical for welded joint properties. Re-crystallization and grain growth were observed in HAZ where its width is slightly increased with increasing welding current due to higher heat input. However, a reasonable HAZ width was observed in all cases.

Optical micrographs of cross sections taken from butt welded joint made using ~~125~~ 100A welding current, 14V welding voltage, 135mm/min welding speed, 15 l/min argon shielding and different oxygen contents in purging gas (0.05, 0.5%) are shown in Figures 21, 22 respectively. The noticeable feature is the directional nature of the austenitic microstructure around weld center of both welded joints. No solidification cracking was found in the weld zone. Structures of weld metal in both joints were almost similar. A dendritic microstructure was developed at fusion boundary due to fast cooling conditions (Figures 21-c, 22- c). More globular structures were observed

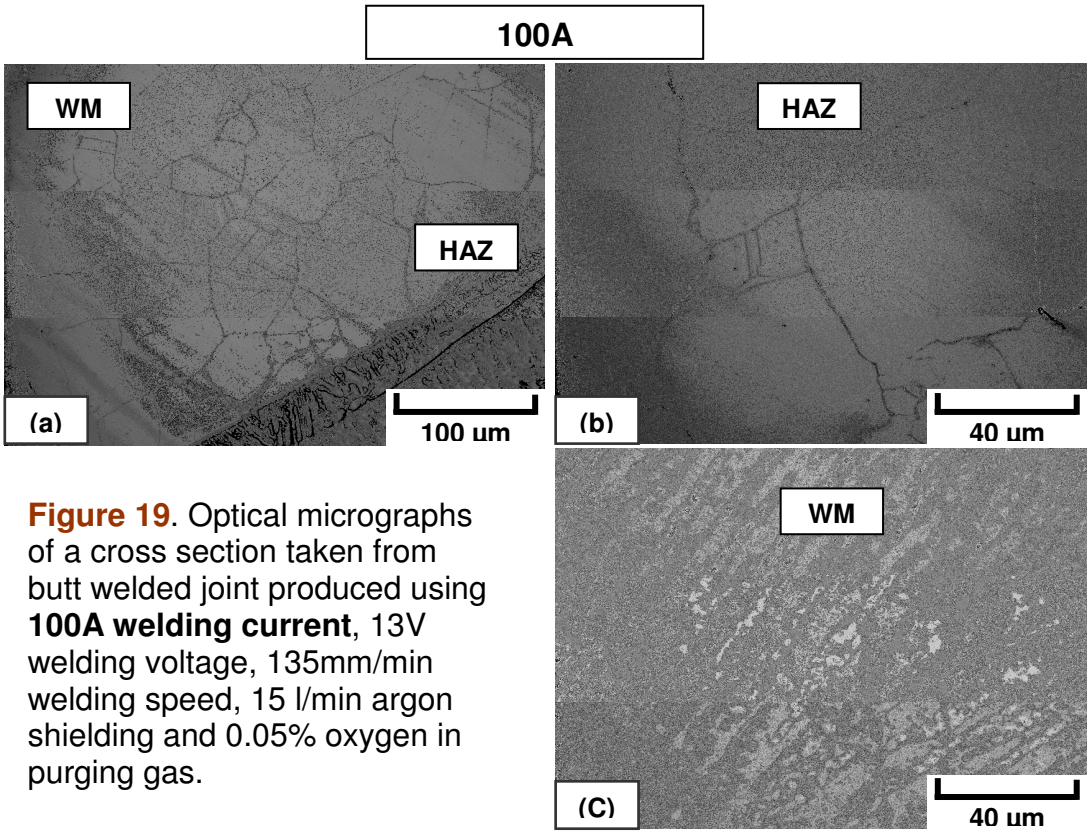

Figure 19. Optical micrographs of a cross section taken from butt welded joint produced using **100A welding current**, 13V welding voltage, 135mm/min welding speed, 15 l/min argon shielding and 0.05% oxygen in purging gas.

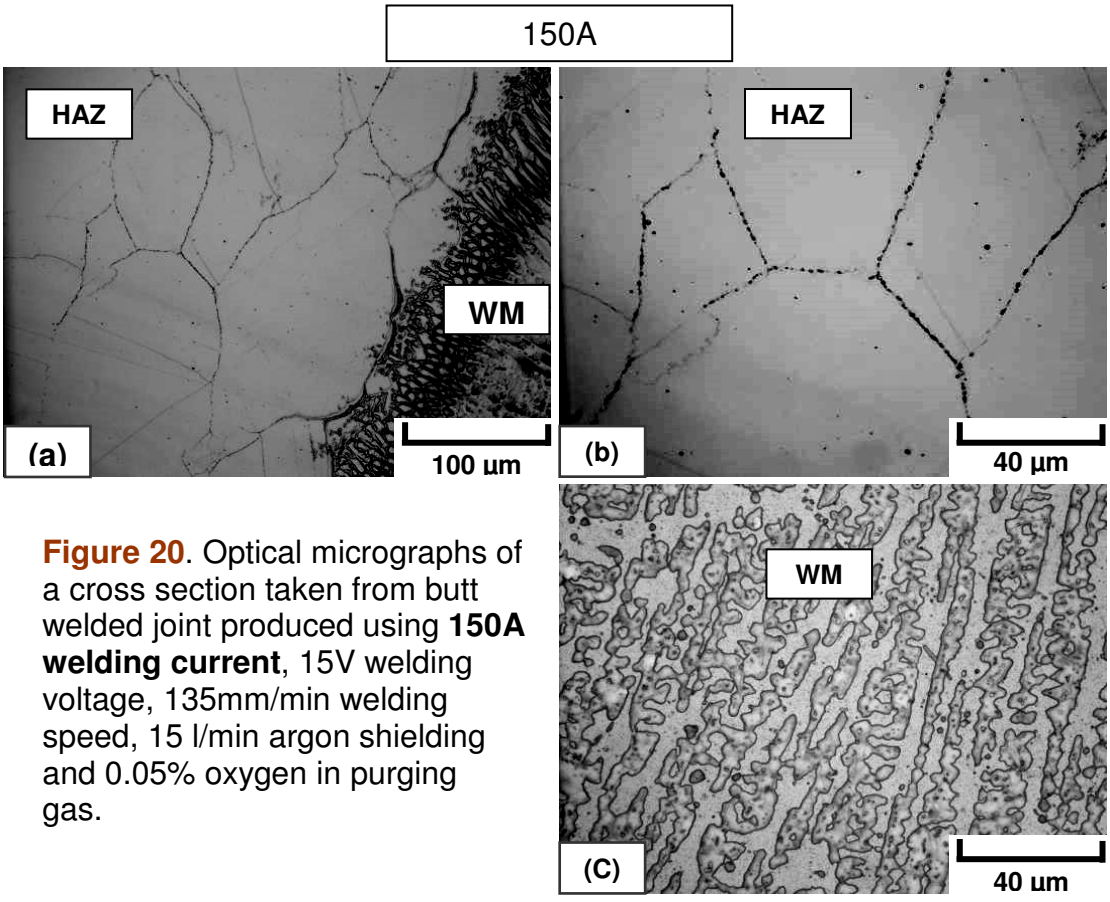

Figure 20. Optical micrographs of a cross section taken from butt welded joint produced using **150A welding current**, 15V welding voltage, 135mm/min welding speed, 15 l/min argon shielding and 0.05% oxygen in purging gas.

at weld metal center that exposed to lower cooling rates and with a less pronounced heat flow direction. In general, the higher the oxygen content in purging gas, the coarser is the dendritic structure, particularly at weld root side due to decreasing cooling rate as a result of higher heat input.

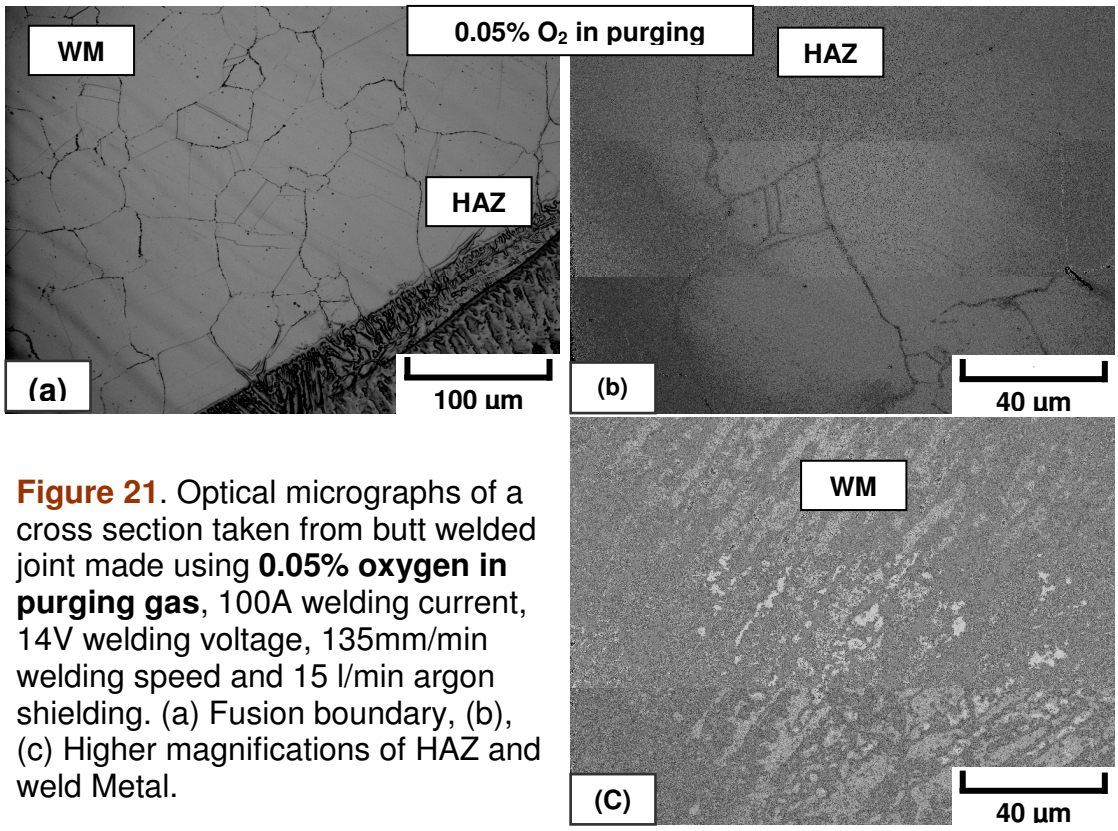

Figure 21. Optical micrographs of a cross section taken from butt welded joint made using **0.05% oxygen in purging gas**, 100A welding current, 14V welding voltage, 135mm/min welding speed and 15 l/min argon shielding. (a) Fusion boundary, (b), (c) Higher magnifications of HAZ and weld Metal.

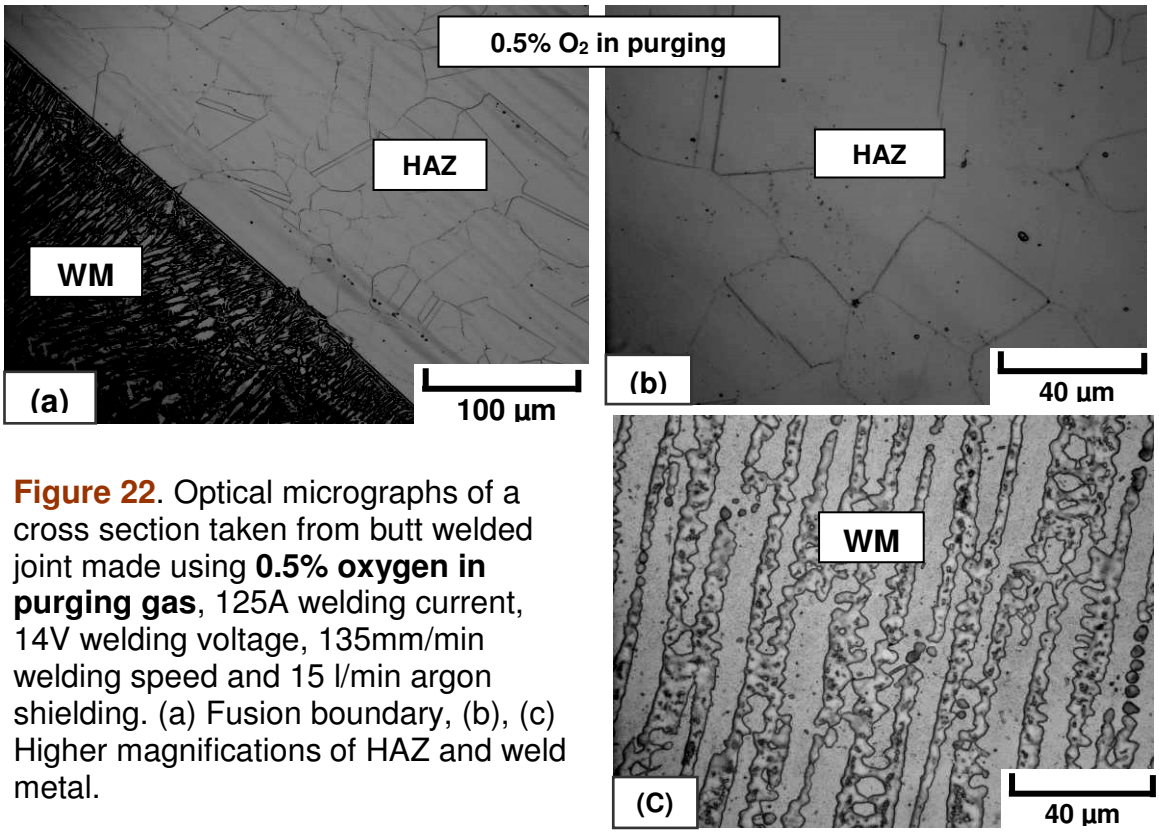

Figure 22. Optical micrographs of a cross section taken from butt welded joint made using **0.5% oxygen in purging gas**, 125A welding current, 14V welding voltage, 135mm/min welding speed and 15 l/min argon shielding. (a) Fusion boundary, (b), (c) Higher magnifications of HAZ and weld metal.

Regarding heat affected zone (HAZ) microstructure, re-crystallization and grain growth were observed in HAZ while its width is slightly increased with increasing oxygen content in purging gas, particularly at weld root side due to higher heat input as a result of exothermic reaction. In general, a reasonable HAZ width was observed in both cases. Generally, the effect of oxygen content in purging gas on microstructure is relatively less than that of the welding current.

Hardness profile through WM, HAZ and BM of butt welded joints made using 135mm/min welding speed, 15 l/min argon shielding, 0.05% oxygen in purging gas and different welding currents (100, 125, 150A) is shown in Figure 23. The results reveal that welding current has no significant effect on hardness values of both WM and HAZ. Generally, hardness values of WM and HAZ are close to that of base metal. This is attributed mainly to low heat input in case of GTAW process as well as the nature of the used superaustenitic stainless steel, which is not susceptible to hardnening during heat treatment. In other words, no significant difference between hardness of the base metal and that of weld metal or HAZ was observed regardless of welding current. This is expected because mechanical properties of austenitic stainless steel, in general, are based on its microstructure that was not remarkably changed**.**

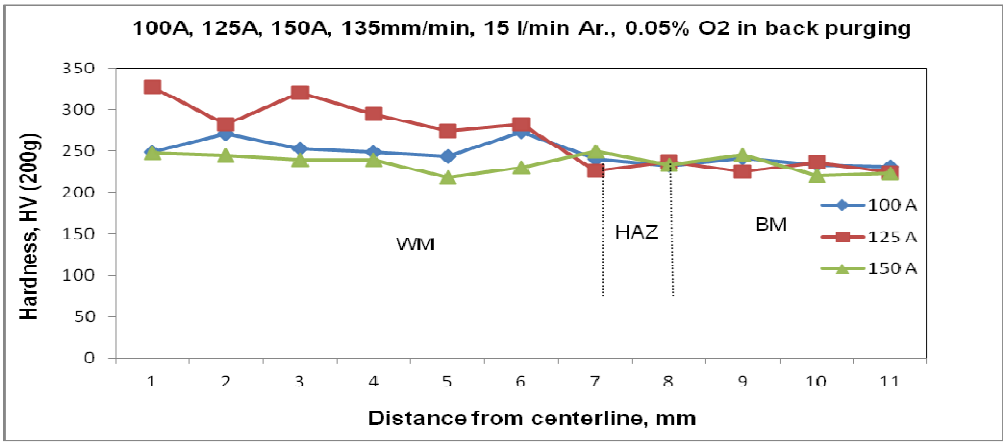

Figure 23. Comparison of hardness profiles through WM, HAZ and BM of butt welded joints made using **different welding currents**, 135mm/min welding speed and 0.05 % oxygen in purging gas.

Comparison of hardness profiles through WM, HAZ and BM of butt welded joints made using 125A welding current, 14V welding voltage, 135mm/min welding speed, 15 l/min argon shielding and different oxygen contents in purging gas (0.05, 0.5%) is summarized in Figures 24. The results of hardness measurements reveal that oxygen content in purging gas has no significant effect on hardness values of both WM and HAZ. Generally, hardness values of WM and HAZ are close to that of base metal. This is attributed mainly to low heat input in case of GTAW process as well as the nature of the used superaustenitic stainless steel, which is not susceptible to hardnening during heat treatment. In other words, no significant difference between hardness of the base metal and that of both weld metal or HAZ was observed regardless of oxygen content in purging gas. This is expected because mechanical

properties of austenitic stainless steel, in general, are based on its microstructure that was not remarkably changed**.**

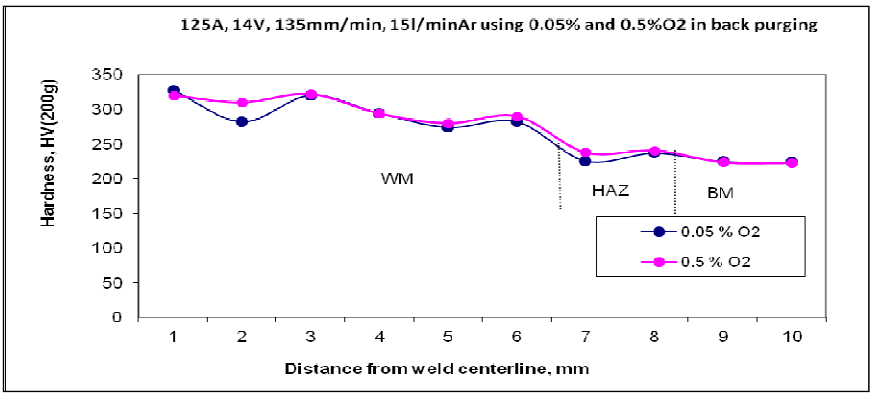

Figure 24. Hardness profile through WM, HAZ and BM of butt welded joint produced using **different oxygen contents in purging gas**, 125A welding current, 14V welding voltage, 135mm/min welding speed and 15 l/min argon shielding.

Mechanical Properties of Butt Welded Joints

Results of both face and root bend tests of all welded joints showed no cracking after U-bend was made. Results of tensile test of butt welded joints made using 135mm/min, 15 l/min argon shielding and different welding currents (100, 125, 150A), as well as that of base metal and standard material are summarized in Figure 25. The given values of tensile properties are the average of two readings. The tensile fracture was occurred either in HAZ or weld metal of all welded joints. However, the obtained tensile strength of all welded joints is higher than that specified minimum tensile strength for base metal. This means that the obtained tensile strength of all welded joints is satisfactory and accepted since it meets the requirements of the concerned standard (API 570). It indicates that tensile test for welding procedure qualification is passed if failure occurred either in weld metal at strength >= that of specified minimum tensile strength for base metal or in base metal. It can be noticed that the tensile strength of welded joint is not significantly affected by welding current since the used base metal is not susceptible to hardening due to heat treatment or welding.

Results of tensile test of butt welded joint made using 125A, 14V, 135mm/min, 15 l/min argon shielding and different oxygen contents in purging gas (0.05, 0.5%) as well as that of base metal and standard material are summarized in Figure 26. The given values of tensile properties are the average of two readings. The tensile fracture was occurred either in HAZ or weld metal of all welded joints. However, the obtained tensile strength of all welded joints is higher than that specified minimum tensile strength for base metal. This means that the obtained tensile strength of all welded joints is satisfactory and accepted since it meets the requirements of the concerned standard for engineering applications as mentioned above. It can be noticed that the tensile strength of welded joint is not significantly affected by oxygen

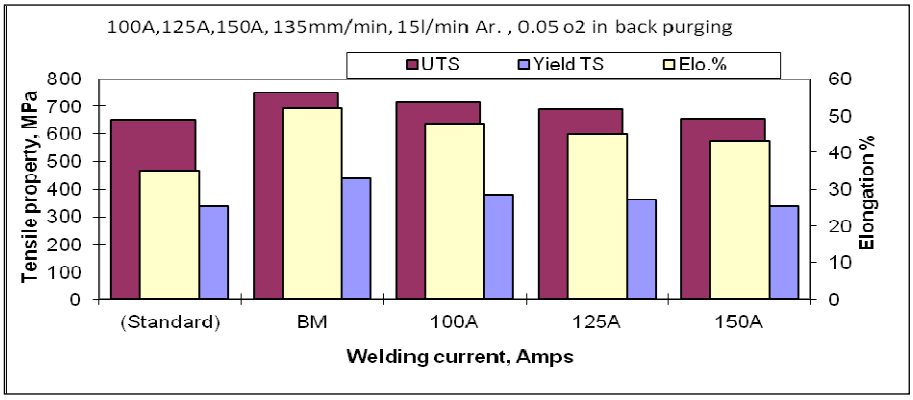

Figure 25. Tensile properties of butt welded joints as a function of welding current together with that of base metal and standard material.

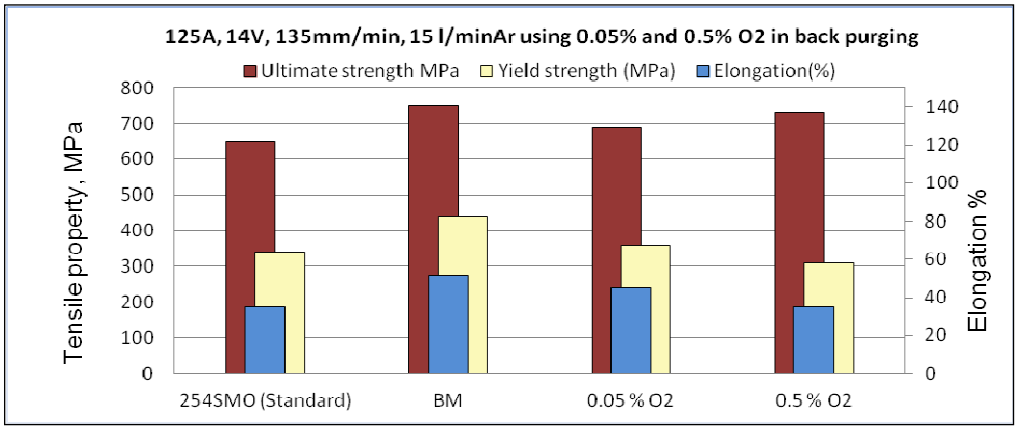

Figure 26. Tensile properties of butt welded joints of as a function of oxygen content in purging gas.

contents in purging gas since the used base metal is not susceptible to hardening due to heat treatment or welding.

Corrosion Properties of Butt Welded Joints

Based on Tafel Polarisation data, corrosion rate, corrosion resistance, current density and corrosion potential open circuit were obtained for different welded joints as well as for the used base metal. Corrosion rate of GTA welded joints made using different welding currents in comparison with that of base metal are shown in Figure 27. It is found that corrosion rate of welded joint increases with the increase in welding current as the welding area increases. In addition, it is noticed that increasing the welding current caused a significant increase in corrosion rate. This may attribute to increasing fusion zone area with increasing welding current. Usually, the rate of corrosion increases with the increase in fusion zone size. GTA welded joint made using lower welding current with its smaller fusion zone size did not have the highest percentage weight loss in comparison with that made using higher welding current. Because the base metal corrosion was negligible, the weight loss is limited by the amount of weld metal available for corrosion.

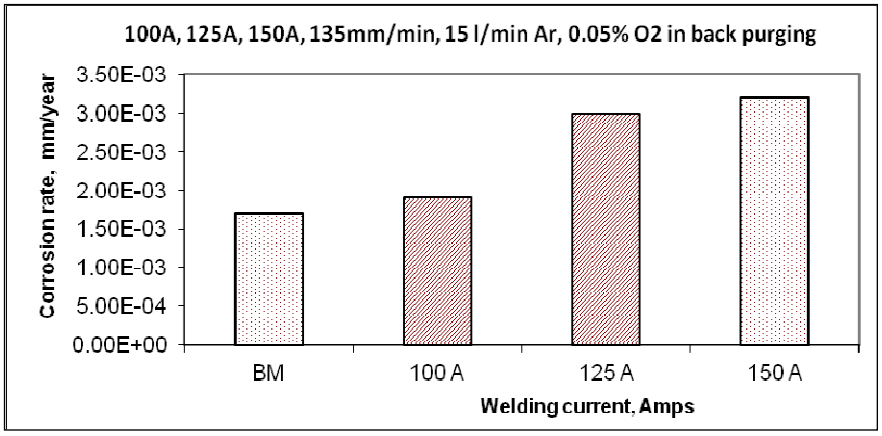

Figure 27. Comparison of corrosion rate of GTA welded joints made using different welding currents in comparison with that of base metal.

Corrosion resistance of GTA welded joints made using different welding currents in comparison with that of base metal are shown in Figure 28. It is found that corrosion resistance of welded joint decreases with the increase in welding current as the welding area increases. In other words, increasing the welding current causes a significant decrease in corrosion resistance of welded joint. This is attributed to increase in fusion zone area with increasing welding current. Usually, the rate of corrosion increases with the increase in fusion zone size. GTA welded joint made using lower welding current with its smaller fusion zone size did not have the highest percentage weight loss in comparison with that made using higher welding current. Because the base metal corrosion was negligible, the weight loss is limited by the amount of weld metal available for corrosion.

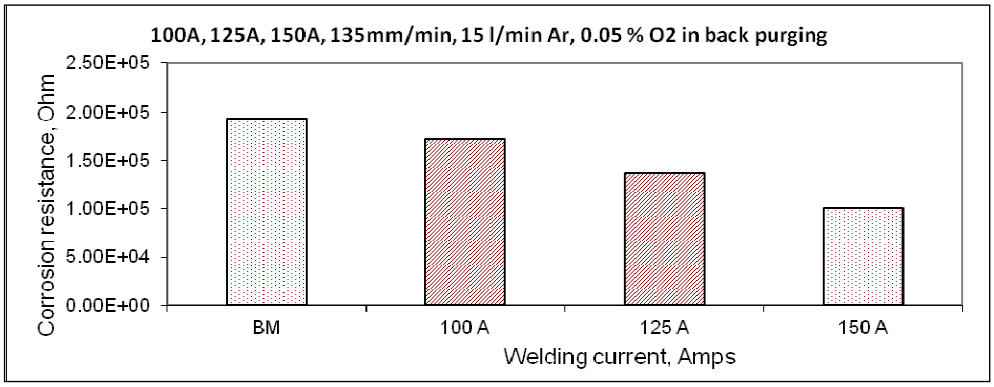

Figure 28. Comparison between the corrosion resistance of GTA welded joints made using different welding currents.

Corrosion rate of GTA welded joints as a function of different oxygen contents in purging gas is shown in Figure 29. It is found that corrosion rate of welded joint increases with the increase in oxygen content in purging gas. This is attributed to relatively higher heat input as well as existence of oxidation at root side.

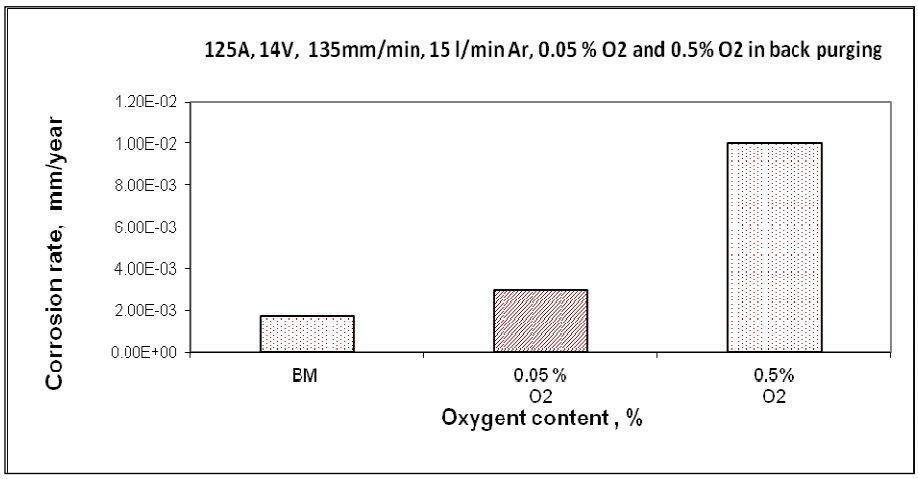

Figure 29. Comparison between corrosion rates of GTA welded joints made using different oxygen contents in purging gas.

In other words, welded joint made using lower oxygen content in purging gas with smaller fusion zone size has better corrosion resistance in comparison with that produced using higher oxygen content in purging gas. Because the base metal corrosion was negligible, the weight loss is limited by the amount of weld metal available for corrosion.

Comparison of the corrosion resistance of GTA welded joints made using different oxygen contents in purging gas is shown in Figure 30. It is found that corrosion resistance of welded joint decreases with the increase in oxygen content in purging gas. This is attributed to larger weld zone due to higher heat input, as well as increasing oxidation in case of higher oxygen content in purging gas.

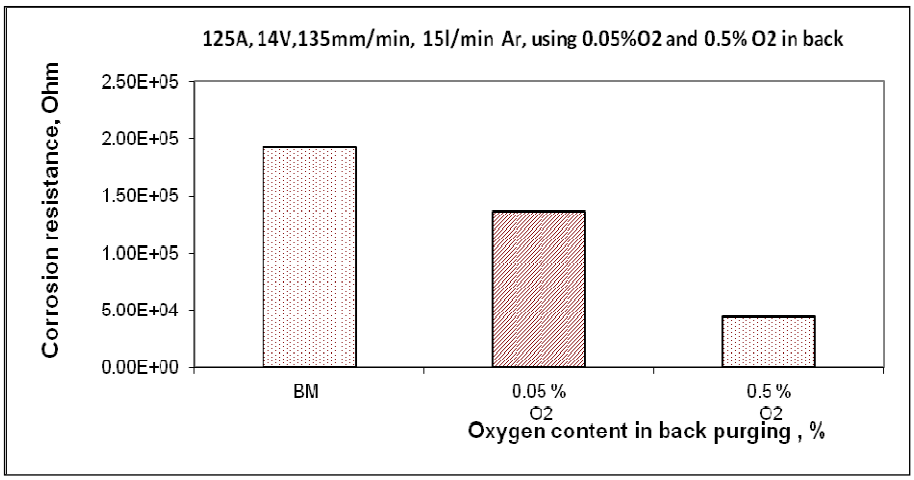

Figure 30. Corrosion resistance of GTA welded joints made using different oxygen contents in purging gas.

CONCLUSION

Based on the results achieved in this investigation it can be concluded that welding parameters played an important role in obtaining acceptable weld profile. Lower welding current and/or lower oxygen content in purging gas resulted in better weld profile with smaller weld zone due to lower heat input. Besides, acceptable mechanical and corrosion properties were obtained in comparison with that of base metal.

Mechanical propertied of GTA welded joints were not significantly affected by either welding current or oxygen content in purging gas since the used base metal is not susceptible to hardening due to welding.

On the other hand, corrosion rate increased with the increase in welding current and/or oxygen content in purging gas. This is related to the increase in weld zone size due to higher heat input in this case. This means that GTA welded joint made using lower welding current and/or lower oxygen content in purging gas with smaller fusion zone size has better mechanical properties as well as corrosion resistance. This welded joint did not have the highest loss in mechanical and corrosion properties, in comparison with that made using higher welding current and/or oxygen content in purging gas. Because the base metal corrosion was negligible, the weight loss is limited by the amount of weld metal available for corrosion.

REFERENCES

[1] Engineering Encyclopedia Saudi Aramco DeskTop Standards, File Reference: PCI20402, Courses, December 2006.

[2] S. Heino, E. M. Knutson-Wedel, and B. Karlsson, Precipitation behavior in heat affected zone of welded superaustenitic stainless steel δγ, Material Science and Technology January 1999 Vol. 15.

[3] Mats L., Avesta S.A.B., Development of Superaustenitic Stainless Steels, Welding in the World, Vol.36, pp.55-63, 1995.

[4] Cleiton Carvalho Silva, Jesualdo Pereira Farias, Hosiberto Batista de Sant'Ana, Evaluation of AISI 316L stainless steel welded plates in heavy petroleum environment (1), 2008 Elsevier Ltd.

[5] E.A. Abd El Meguid *, A.A. Abd El Latif, Electrochemical and SEM study on Type 254 SMO stainless steel in chloride solutions.

[6] E.A. Abd El Meguid *, A.A. Abd El Latif, Critical pitting temperature for Type 254 SMO stainless steel in chloride solutions, 2006 Elsevier Ltd.

[7] Sandvik 254 SMO S-1884-ENG April 1999 STAINLESS - stainless steels and their properties.

[8] L. Reclaru, R. Lerf, P.-Y. Eschler, J.-M. Meyer, Corrosion behavior of a welded stainless-steel orthopedic implant, Biomaterials 22 (2001) 269– 279.

[9] T. D. Anderson, M. J. Perricon, J. N. Dupont, and A. R. Marder, The Influence of Molybdenum on Stainless Steel Weld Microstructures (14), Welding Journal, Sep. 2007, Vol. 86, p-281.

[10] M. Dadfar, M.H. Fathi, F. Karimzadeh, M.R. Dadfar, A. Saatchi,Effect of TIG welding on corrosion behavior of 316L stainless steel(4), 2006 Elsevier B.V.

[11] Stjepan Kožuh, Mirko Gojić, Ladislav Kosec, The effect of annealing on properties of AISI 316L base and weld metals (13), Scientific paper, RMZ – Materials and Geoenvironment, Vol. 54, No. 3, pp. 331-344, 2007.
[12] Ayo Samuel Afolabi, Effect of Electric Arc Welding Parameters on Corrosion Behaviour of Austenitic Stainless Steel in Chloride Medium (5), AU J.T. 11(3): 171-180 (Jan. 2008).
[13] SAES-W-016 , Welding of Special Corrosion-Resistant Materials, 30 March 2005.
[14] Lippold J.C. and Kotecki D.J., Welding Metallurgy and Weldability of Stainless Steels, Wiley &Sons, INC.,pp. 142-151,2005.
[15] Jean-Pierre A., Michel V., and John G., *Corrosion Performance and Field Experience with Super Duplex and Super Austenitic Stainless Steels in FGD Systems, N.A. 2000.*
[16] Saudi Aramco Specification SAES-L-132 material selection for piping system, October, 2005.